Oncology Research, Vol. 25, pp. 511–522
Printed in the USA.

0965-0407/17 $90.00 + .00
DOI: https://doi.org/10.3727/096504016X14756226781802
E-ISSN 1555-3906
www.cognizantcommunication.com

Overexpression of Interferon Regulatory Factor 7 (IRF7) Reduces Bone Metastasis of Prostate Cancer Cells in Mice

Yang Zhao, Wenxia Chen, Weiliang Zhu, Hui Meng, Jie Chen, and Jian Zhang

Department of Oncology, Southern Medical University Affiliated Zhujiang Hospital, Guangzhou, P.R. China

The purpose of this study was to identify the role of interferon regulatory factor 7 (IRF7) in the bone metastasis of prostate cancer. Herein we demonstrated the lower expression of IRF7 in bone metastases of prostate cancer. Overexpression of IRF7 in prostate cancer cells had a marked effect on inhibiting bone metastases but not on tumor growth in xenograft nude mice. While in vitro, upregulation of IRF7 had little effect on the malignant phenotype of prostate cancer cells including proliferation, apoptosis, migration, and invasion. However, prostate cancer cells overexpressing IRF7 significantly enhanced the activity of NK cells, which resulted in the cytolysis of prostate cancer target cells. The underlying mechanism may be relevant to the increasing expression of IFN-β induced by IRF7, as the downregulation of which could inversely inhibit the activity of NK cells. In conclusion, our findings indicate that IRF7 plays a role in reducing bone metastasis of prostate cancer by IFN-β-mediated NK activity.

Key words: Interferon regulatory factor 7 (IRF7); Prostate cancer; Bone metastasis

INTRODUCTION

Prostate cancer causes substantial morbidity and mortality worldwide and remains the second most common cancer in older men[1]. Patients with localized prostate cancer have a relatively long-term survival rate due to great advances in surgical resection and adjuvant therapy. However, patients with advanced, especially metastatic, bone disease are often associated with a poor prognosis. Studies have shown that around 30% of these patients will develop distant metastases within 5 years of diagnosis, even after radical surgery[2]. Bone metastases occur in more than 80% of cases of advanced-stage prostate cancer, which confers a high level of morbidity, with a 5-year survival rate of 25% and a median survival of approximately 40 months[3]. Therefore, studies on an efficient marker for predicting bone metastases of primary prostate cancer will help to identify high-risk patients who may benefit from appropriate therapeutic approaches in order to decrease the risk of bone metastasis.

Interferon regulatory factor 7 (IRF7), one of the most important interferon regulatory factor members, is essential for the induction of type I interferon (IFN)[4] and is highly involved in suppressing cancers. Overexpression of IRF7 in immortal Li–Fraumeni fibroblasts was linked to inhibition of growth and induction of senescence[5]. In the activated B-cell-like subtype of diffuse large B-cell lymphoma[6] and breast cancer[7], IRF7 was also associated with favorable features. Notably, in the breast cancer cell line 4T 1.2, upregulation of IRF7 induced a higher expression of IFN-α and bone metastasis was inhibited in the mouse model for spontaneous breast cancer. By using publicly available gene expression datasets, the IRF7 signature was confirmed to be significantly associated with bone metastases-free survival, with low expression of the IRF7 gene set being associated with a higher number of bone metastatic events[8]. These limited reports demonstrated that the IRF7 gene was a cancer suppressor gene, which may be closely involved in inhibiting bone metastasis. On the contrary, recent studies on glioma showed that high expression of IRF7 was associated with enhanced invasion and poor prognosis[9,10], indicating that IRF7 may be a potential oncogene. However, the role of IRF7 in human prostate cancer has been scarcely understood.

In order to clarify the role of IRF7 in prostate cancer, the prostate specimens were tested. IRF7 was stably overexpressed in two prostate cancer cell lines (PC-3/IRF7 and LnCap/IRF7), and the effects of IRF7 upregulation on these cells were assessed both in vivo and in vitro. Furthermore, the possible mechanisms were also investigated.

Address correspondence to Jian Zhang, Department of Oncology, Southern Medical University Affiliated Zhujiang Hospital, 253 Gongye Road, Guangzhou 510282, P.R. China. E-mail: blacktiger@139.com

MATERIALS AND METHODS

Sample Collection

The human prostate specimens were obtained from the Department of Pathology, Zhujiang Hospital (Southern Medical University, Guangzhou, P.R. China) between the years 2006 and 2009. The specimens consisted of 10 cases with nodular hyperplasia, 82 cases with primary prostate cancer, and 20 cases with bone metastases. The experimental procedures complied with the standards of the Declaration of Helsinki. The study involving human tissue blocks began with the understanding and written agreement of each patient and was approved by the Southern Medical University Faculty Human Ethics Committee.

Immunohistochemistry

Human prostate tissues were deparaffinized and rehydrated routinely. After blocking with endogenous peroxidase blocking solution, the tissue sections were incubated with primary antibody specific to IRF7 (1:100; Santa Cruz Biotechnology, Santa Cruz, CA, USA) at 4°C overnight. After being washed three times with PBS, the tissue sections were incubated with horseradish peroxidase-conjugated anti-rabbit IgG (SV0002; Boster, Pleasanton, CA, USA) according to the manufacturer's instructions. Diaminobenzidine (DAB) was then used for staining. Brown-yellow granules in the nucleus and cytoplasm were regarded as positive staining. The percent positivity of cells stained was scored as 0 if <5% (negative), 1 if <5%–30% (sporadic), 2 if <30%–70% (focal), and 3 if >70% (diffuse), while staining intensity was scored as 0 if no staining, 1 if weakly to moderately stained, and 2 if strongly stained. The IRF7 protein expression levels were classified semiquantitatively on the basis of total scores of the percent positivity and the staining intensity as follows: "IRF7 negative" if the sum scored 0, "IRF7 weak" if the sum scored 1 (+), "IRF7 moderate" if the sum scored 2–3 (++), and "IRF7 high" if the sum was 4–5 (+++)[11]. Each sample was scored by two pathologists who were unaware of the clinical diagnosis.

Cell Culture and Transfection

Human prostate cancer cell lines, PC-3 and LnCap, were obtained from the cell bank of Sun Yat-Sen University (Guangzhou, P.R. China). Cells were cultured in RPMI-1640 medium (GIBCO, Rockville, MD, USA) containing 10% new bovine serum, penicillin, and streptomycin at 37°C in an atmosphere of 5% CO_2. Unless otherwise stated, human natural killer (NK) cells were purified as previously described[12] and cultured in RPMI-1640 medium supplemented with 10% fetal bovine serum, 1% penicillin and streptomycin, and 300 U/ml of human recombinant interleukin-2 (IL-2) (ACRO Biosystems, Beijing, P.R. China) at 37°C in an atmosphere of 5% CO_2.

The coculture system contained NK and prostate cancer cells plated in a six-well round-bottom plate. The effector and target cells were cultured together at ratios of 10:1, with the same number of effector cells in each well (1×10^6 cells per well). The total volume of medium in each well was adjusted to 2 ml. Cells were incubated at 37°C for 24 h, and the conditioned medium was further used to assess the activity of NK cells.

For the establishment of IRF7 overexpression cell lines, PC-3 and LnCap cells were stably transfected with LV5 (EF-1aF/GFP) IRF7 or LV5 (EF-1aF/GFP) IRF7/NC, which were obtained from GenePharma Co. Ltd. (Shanghai, P.R. China). Stable cells were selected by puromycin at the concentration of 1 μg/ml for 14 days. For the transient knockdown of IFN-β in prostate cancer cells, the si-RNA-targeting IFN-β (si-147 and si-623) and negative control si-RNA (si-NC) (GenePharma) were transfected into prostate cancer cells according to the manufacturer's instructions. The si-RNA sequences are listed in Table 1.

RNA Extraction and RT-PCR Analysis

Total RNA was extracted from prostate cancer cells. Reverse transcription reactions were performed for 15 min at 37°C, followed by 5 s at 85°C for complementary DNA (cDNA) synthesis. Real-time reactions were performed using the SYBR® PrimeScript™ RT-PCR Kit (Takara Biotechnology, Dalian, P.R. China) under the following conditions: 30 s at 95°C for 1 cycle, 5 s at 95°C, 20 s at 60°C for 40 cycles, 95°C for 0 s, 65°C for 15 s, and 95°C for 0 s for melting curve analysis. The relative mRNA expression of each gene was calculated based on the comparative expression level $2^{-\Delta\Delta}$Ct method. The primers are listed in Table 2.

Table 1. Information on IFN-β si-RNA Sequence

Sequence Information	
147	Sense 5′-GCUCUUUCCAUGAGCUACATT-3′
	Antisense 3′-UGUAGCUCAUGGAAAGAGCTT-5′
623	Sense 5′-CAUUAACAGACUUACAGGUTT-3′
	Antisense 3′-ACCUGUAAGUCUGUUAAUGTT-5′
NC	Sense 5′-UUCUCCGAACGUGUCACGUTT-3′
	Antisense 3′-ACGUGACACGUUCGGAGAATT-5′

Western Blot Analysis

Cell proteins were extracted with cold RIPA lysis buffer and measured by the standard BCA method (BCATM Protein Assay Kit; Pierce, Rockford, IL, USA). Each protein sample was homogenized in the loading buffer, boiled for 15 min, and electrophoresed on a 10% polyacrylamide gel (SDS-PAGE), then transferred to a polyvinylidene difluoride (PVDF) membrane (Millipore, Billerica, MA, USA). After being blocked with 5% BSA for 2 h, the membrane was treated with primary antibodies specific to IRF7 (1:1,000; Santa Cruz Biotechnology) and GAPDH (1:10,000; EarthOx, Beijing, P.R. China) overnight at 4°C. The membranes were washed again with TBST [10 mM Tris (pH 8.0), 150 mM NaCl, and 0.1 Tween 20], followed by incubation with horseradish peroxidase-labeled secondary antibody (Biosynthesis Biotechnology Co., Ltd., Beijing, P.R. China) for 1 h at room temperature and then stained with super echochemiluminescence (ECL) plus detection reagents. The protein bands of membranes were visualized by exposure to X-ray film. The intensity of the protein bands was quantified by the Quantity One software (Bio-Rad, Hercules, CA, USA). GAPDH was used as a control in the experiments.

Enzyme-Linked Immunosorbent Assay

To measure the cytokine production of cultured cells, culture supernatant was collected. The levels of IFN-β and perforin-1 in the supernatant were measured using the human IFN-β and perforin-1 ELISA kit (CUSABIO, Wuhan, P.R. China) according to the manufacturer's instructions. Recombinant IFN-β and perforin-1 were used to generate a standard curve, which was employed in calculating the IFN-β and perforin-1 concentrations of all samples.

LDH Release Assay

LDH assay was performed to assess the LDH release of prostate cancer cells. The coculture system, NK and prostate cancer cells, was cultured with complete medium or the supernatant of prostate cancer cells overexpressing IRF7 for 24 h. Then the culture medium was collected, and the intracellular LDH release was measured at an absorbance of 440 nm. The concentration of LDH release (U/L) was calculated as follows: (absorbance at 440 nm in media − absorbance at 440 nm in control)/(standard absorbance at 440 nm − absorbance at 440 nm in blank) × standard sample concentration (2 mmol/L) × $N \times 1{,}000$.

Colony Formation Assay

Prostate cancer cells growing in log phase were plated in a six-well plate. The following day, cells were incubated for 12 days. Next, colonies were washed with PBS, fixed with 4% paraformaldehyde, stained with 0.1% crystal violet, and counted. Colonies consisting of more than 50 cells were counted as surviving colonies. The surviving fraction was calculated as described previously[12].

Flow Cytometry Assay

For analysis of the apoptotic cell population, prostate cancer cells were harvested, washed with PBS, and resuspended in binding buffer containing 7-aminoactinomycin D (BD Pharmingen, San Diego, CA, USA) for 10 min, followed by the addition of APC Annexin-V (BioLegend, San Diego, CA, USA). Cell apoptosis analysis was carried out using a flow cytometer (BD Biosciences, Oxford, UK).

Wound Healing Assay

Cells were seeded on 24-well plates and grown to monolayer. Wound areas were scraped using 100-μl plastic tips. At the indicated times (0, 12, 24, and 48 h), wound areas were photographed, and the wound healing rate was calculated. Healing rate = (width of wound at 0 h − width of the wound at *x* h)/width of wound at 0 h.

Invasion Assay

Using 24-well Transwell units with polycarbonate inserts (8-μm pore size), Matrigel (50 μl) as a basement membrane was spread on the polycarbonate membrane and allowed to solidify for 1 h at room temperature. Cells that were suspended in RPMI-1640 containing 5% BSA were added to each upper compartment of the Transwell

Table 2. Primer Sequences

Name	Forward Primer (5′–3′)	Reverse Primer (5′–3′)
IRF7	CCACACCCCCATCTTCGA	CCTCCGAGCCCGAAACTC
MMP-9	AGTCCACCCTTGTGCTCTTC	ACTCTCCACGCATCTCTGC
VEGF-A	CCAACTTCTGGGCTGTTCTC	CCCTCTCCTCTTCCTTCTCTTC
IL-6	TTCGGTCCAGTTGCCTTCT	GGTGAGTGGCTGTCTGTGTG
P-53	TAGTGTGGTGGTGCCCTATG	CCAGTGTGATGATGGTGAGG
GAPDH	GCACCGTCAAGGCTGAGAAC	TGGTGAAGACGCCAGTGGA
IFN-β	TCTCCTGTTGTGCTTCTCCA	GTCAAAGTTCATCCTGTCCTTG
IFN-α	GAGGAGAGGGTGGGAGAAAC	CAGGCACAAGGGCTGTATTT

units. RPMI-1640 medium containing 30% BSA was then added to each lower compartment of the Transwell units. After being cultured for 48 h, cells that penetrated through the Matrigel-coated polycarbonate membrane were fixed by paraformaldehyde, stained with 0.1% crystal violet, and counted in five randomly chosen fields.

In Vivo Tumorigenicity Assay

Animal experiments were performed using male nude mice (4–6 weeks old, 12–16 g) purchased from the animal facility of Sun Yat-Sen University. The animal facilities and experiments were in accordance with local institutional guidelines for animal welfare and were approved by the animal ethics committee of the Sun Yat-Sen University.

The stable transfected prostate cancer cells (2×10^6) were resuspended in 200 μl of PBS and injected into the caudal vein of recipient mice. At 30 days after injection, mice were anesthetized, and then digital radiographs were taken to monitor the metastatic bone lesions. The animals were euthanized on day 30, and the bone lesions were confirmed by staining sections with hematoxylin and eosin. IFN-β and perforin-1 expression in peripheral blood of nude mice were detected by ELISA.

In addition, cells (5×10^6) were resuspended in 100 μl of PBS and injected subcutaneously into the dorsal right flank of nude mice. The tumor length and width were measured weekly by a sliding caliper. The tumor volumes were calculated using the following equation: $V=(W^2\times L)/2$, where W is the width, and L is the length.

Statistical Analysis

Data were analyzed using the SPSS 20.0 software (Chicago, IL, USA). Results were presented in term of means ± standard deviation (SD). Comparison of means between two samples was performed using Student's *t*-test. Statistical comparisons of more than two groups were performed using one-way analysis of variance (ANOVA), and then multiple comparisons were performed using least significant difference (LSD). The association between IRF7 protein expression and clinical features was analyzed by a Pearson chi-square test. Kaplan–Meier survival analysis was performed. In all cases, $p<0.05$ was considered statistically significant.

RESULTS

Low Level of IRF7 Was Expressed in Bone Metastases and Was Associated With Bone Metastasis in Primary Prostate Cancer

To assess the expression of IRF7 in prostate nodular hyperplasia, primary prostate cancer, and bone metastatic tumors, immunohistochemistry (IHC) analysis of IRF7 expression in the tissues of 112 patients was performed. IRF7 was widely expressed in hyperplasia cases (90%, 9 out of 10) and prostate cancer samples (78%, 64 out of 82), but its expression was almost suppressed in bone metastases (20%, 4 out of 200) (Fig. 1A). The data suggested that suppressed IRF7 expression might be associated with bone metastasis.

However, Kaplan–Meier analysis revealed that low IRF7 expression in prostate cancer tissues was related to distant metastasis compared with the group of high IRF7 expression ($p=0.043$) (Fig. 1B). Notably, after excluding the prostate cancer patients with distant metastasis other than the bone, patients with low IRF7 expression had increased risk of developing bone metastasis instead of viscera ($p=0.030$) (Fig. 1C). Moreover, a low level of IFN-β, which was recommended as a biomarker of biochemical recurrence in prostate cancer, was found more often expressed in metastasis specimens (61.3%) when compared with the nonmetastasis specimens (41.2%, $p=0.077$), but it alone could not predict development of bone metastasis ($p=0.055$). Remarkably, Kaplan–Meier analysis showed that a low level of both IRF7 and IFN-β in prostate cancer tissues could further identify the development of bone metastasis ($p=0.001$) (Fig. 1D). This result demonstrated the clinical importance of IRF7 and IFN-β in human prostate cancer.

Overexpression of IRF7 Suppressed Bone Metastasis In Vivo

To determine the function of IRF7 in prostate cancer bone metastasis, the IRF7 stably overexpressed prostate cancer cells (PC-3/IRF7 and LnCap/IRF7) were constructed. The PC-3/IRF7 and LnCap/IRF7 showed clearly increased IRF7 expression at both the mRNA and protein levels compared with the control cells (Fig. 2A and B). Only three lesions from three out of five mice injected with PC-3/IRF7 cells had detectable metastatic lesions, mainly in the distal femurs and proximal tibias, whereas eight lesions from five out of five mice injected with PC-3/NC showed such metastatic lesions (Fig. 2C). These metastatic lesions were confirmed by hematoxylin and eosin (Fig. 2D). In addition, overexpression of IRF7 resulted in a reduction of tumor burden of PC-3/IRF7 in bone metastases, as confirmed by PCR ($p<0.05$) (Fig. 2E). These results suggested that overexpression of IRF7 could inhibit prostate cancer bone metastasis in vivo.

In addition, the effects of IRF7 on tumor growth in xenograft nude mice were explored. The mean volumes of tumors from PC-3/NC and PC-3/IRF7 were 455.47 ± 18.70 mm^3 and 448.00 ± 43.26 mm^3, and those from LnCap/NC and LnCap/IRF7 were 435.47 ± 31.02 mm^3 and 415.50 ± 38.54 mm^3, respectively, showing that upregulation of IRF7 could not suppress tumor growth in vivo (Fig. 2F).

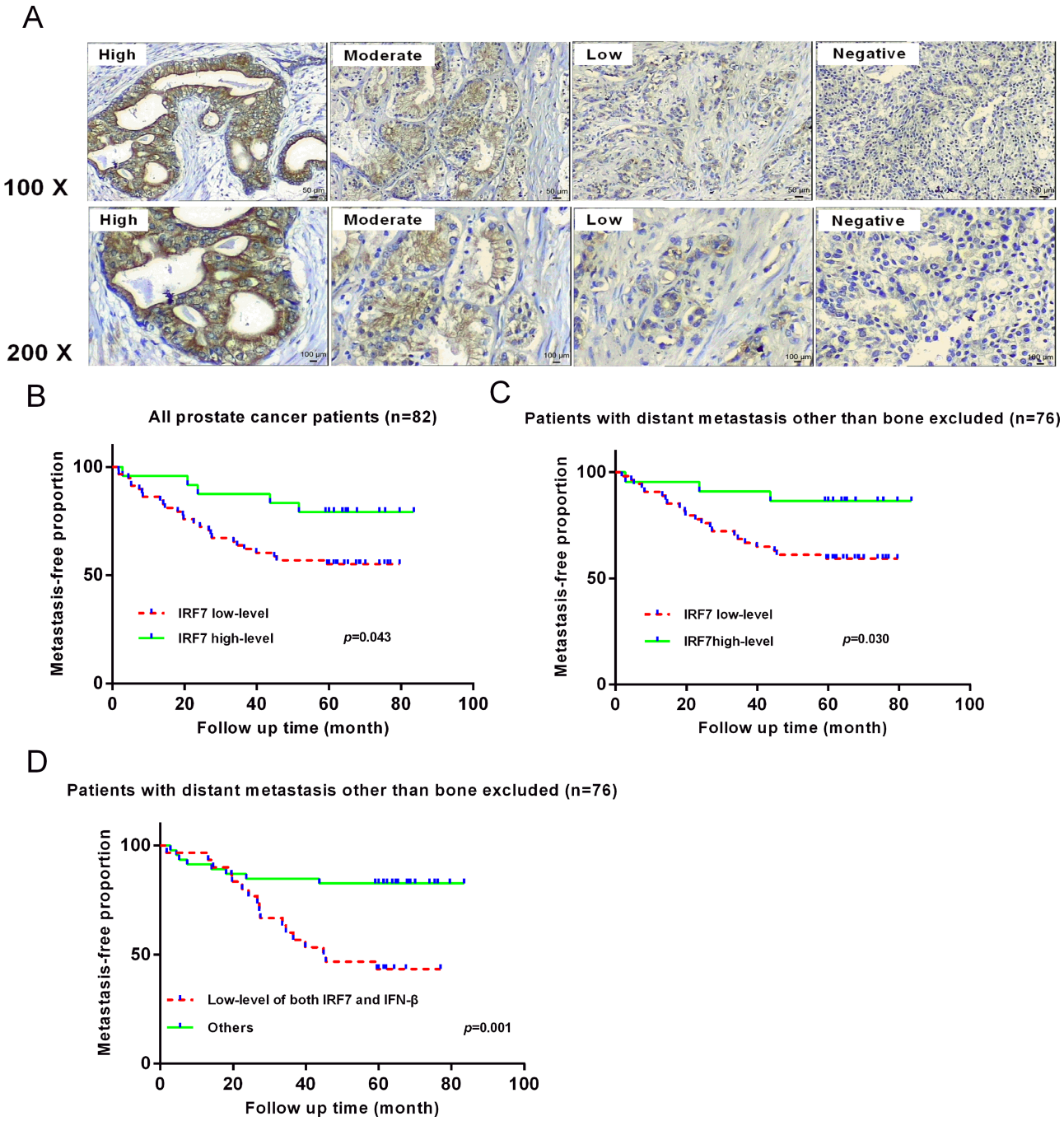

Figure 1. The expression of IRF7 in prostate specimens was detected by immunohistochemistry (IHC). (A) A total of 10 nodular hyperplasia cases, 82 primary prostate cancer cases, and 20 bone metastases were detected using IHC. The pictures show mainly cytoplasmic positivity of IRF7 in prostate tissues. (B) Kaplan–Meier analysis of a low level of IRF7 in primary prostate cancer. Patients with primary prostate cancer expressing a low level of IRF7 were more likely to develop distant metastasis. $p=0.043$. (C) Patients with a low level of IRF7 were more likely to develop distant bone metastasis. $p=0.030$. (D) Kaplan–Meier analysis of a low level of both IRF7 and IFN-β in primary prostate cancer. Patients with a low level of both IRF7 and IFN-β were more likely to develop distant bone metastasis. $p=0.001$.

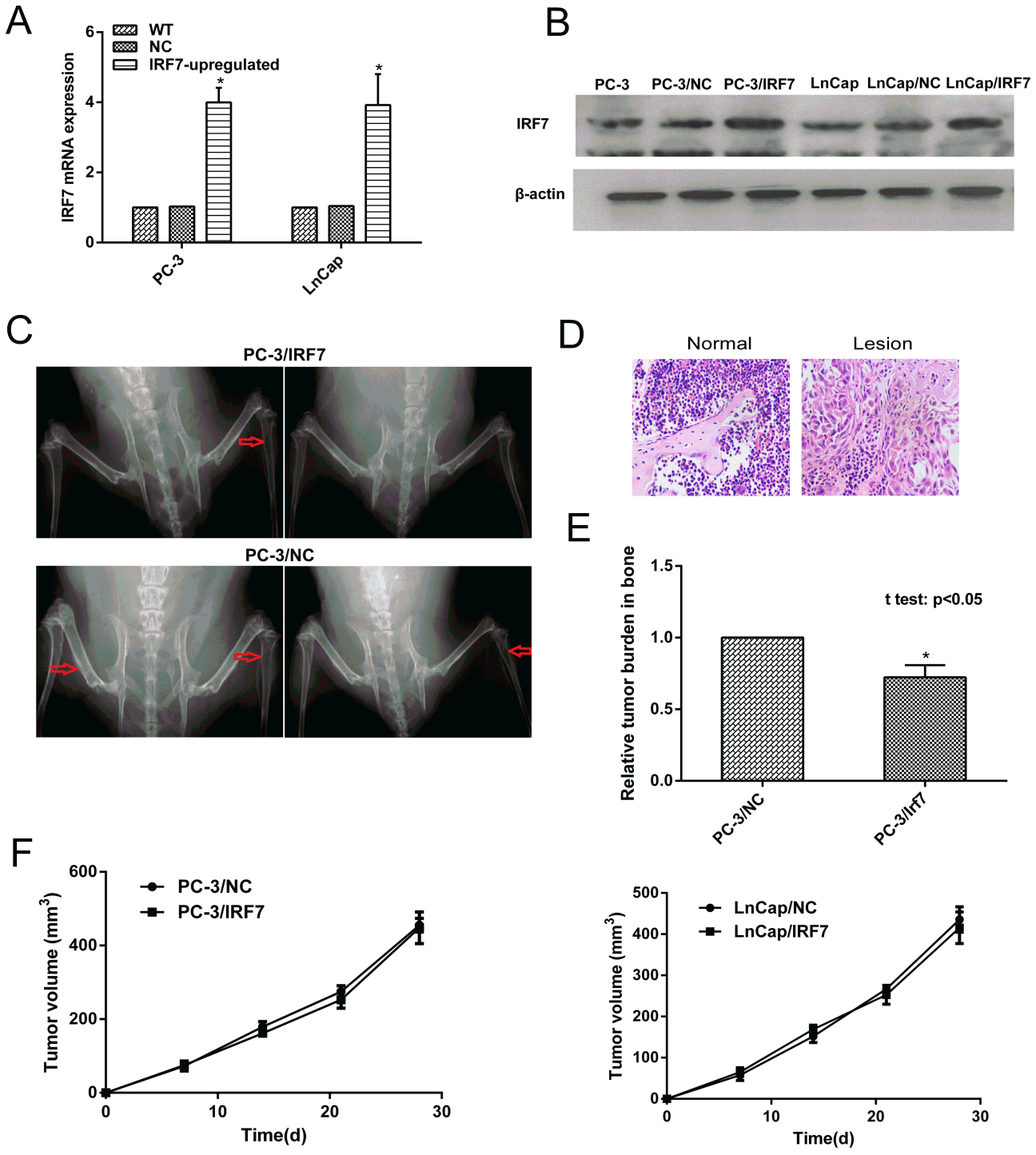

Figure 2. Overexpression of IRF7 inhibited prostate cancer bone metastasis. (A) The expression of IRF7 mRNA was determined by qRT-PCR. The expression of IRF7 mRNA in PC-3/IRF7 and LnCap/IRF7 cells was increased compared with the control cells. (B) The expression of IRF7 protein was determined by Western blot. The expression of IRF7 at the protein level in PC-3/IRF7 and LnCap/IRF7 cells was increased compared with the control cells. (C) PC-3/IRF7 and PC-3/NC cells (2×10^6 per mouse) were injected into the caudal vein of male nude mice. At 30 days after injection, mice were anesthetized, and digital radiographs were taken. The red arrows in the X-ray images show the metastatic bone lesions of PC-3/IRF7 and PC-3/NC cells after injection. (D) The lesions were confirmed by staining sections with hematoxylin and eosin. (E) Quantitative real-time PCR detection against the GFP gene of metastatic tumor burden in bone was conducted. *$p<0.05$. (F) The growth curves of the prostate tumors in xenograft nude mice were constructed.

IRF7 Had Little Effect on the Malignancy of Prostate Cancer In Vitro

To investigate the effect of IRF7 on prostate cancer cells, a series of analyses was conducted in vitro. First, cell proliferation was assessed by the colony formation assay. The result of the colony formation assay showed that PC-3/IRF7 and LnCap/IRF7 cells had similar survival fractions compared with control cells, which had no statistical significance ($p > 0.05$) (Fig. 3A). The apoptosis rates of cells were analyzed using flow cytometry, but IRF7 overexpression did not alter the apoptosis rates of cells in vitro ($p > 0.05$) (Fig. 3B). The wound healing

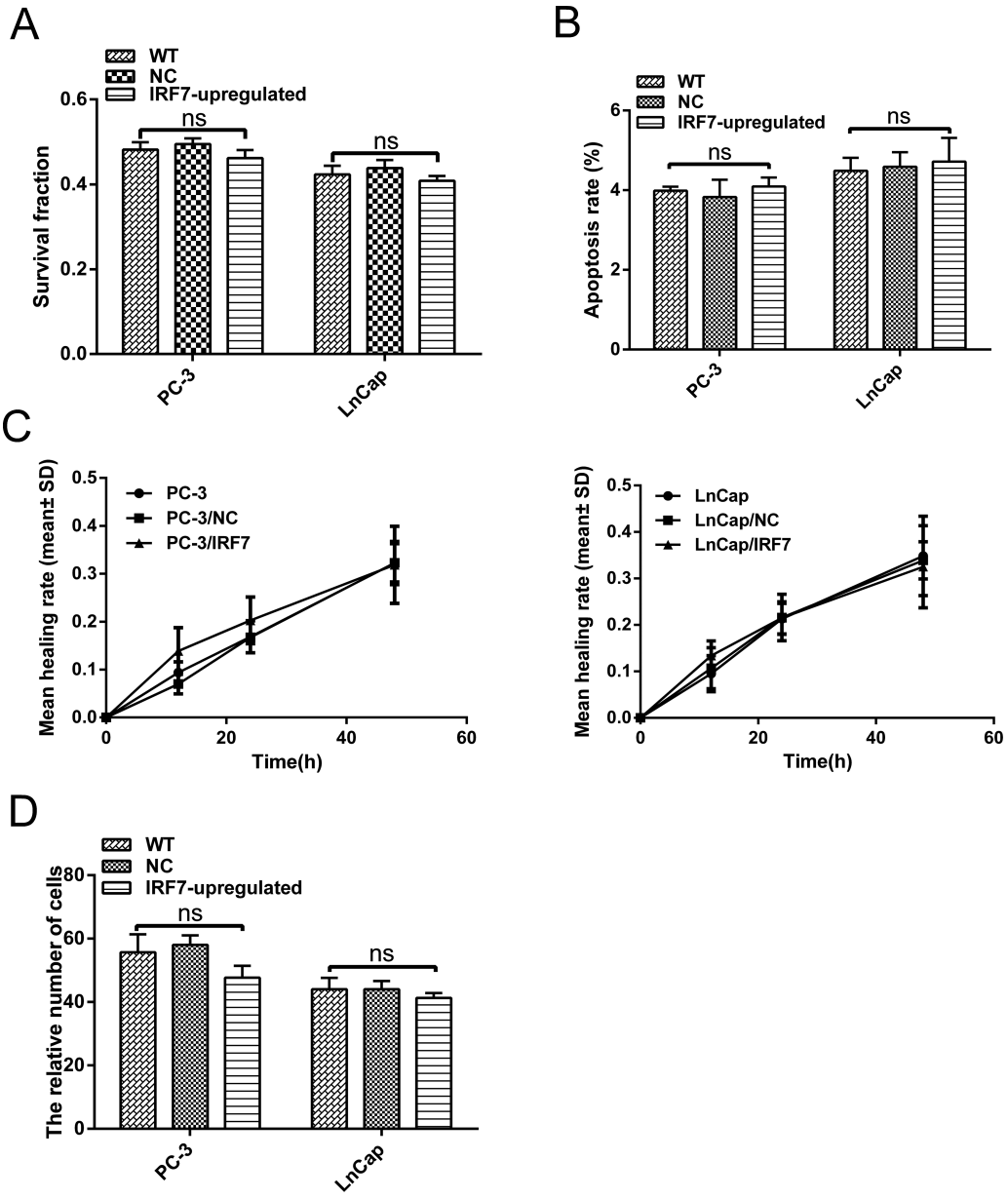

Figure 3. Effect of IRF7 on the malignancy of prostate cancer in vitro. (A) The colony formation assay of prostate cancer cells. Survival fractions were calculated for each group. Representative images of clones and quantitative analysis of survival fraction in the groups are shown. (B) The cell apoptosis rate was measured using a flow cytometer. Representative images of apoptosis and quantitative analysis of apoptosis rate in the groups are shown. $p > 0.05$. (C) Migration ability of PC-3 and LnCap cells was studied by scratch wound assay. The healing rate = (the width of the wound at 0 h − the width of the wound at x h)/the width of the wound at 0 h. Data are presented as mean ± SD. $p > 0.05$. (D) Cell invasion assay was applied to compare invasion abilities. Cells were seeded on the upper side of the Matrigel-coated membrane. The cells penetrating the Matrigel-coated membrane were counted. ns, not significant.

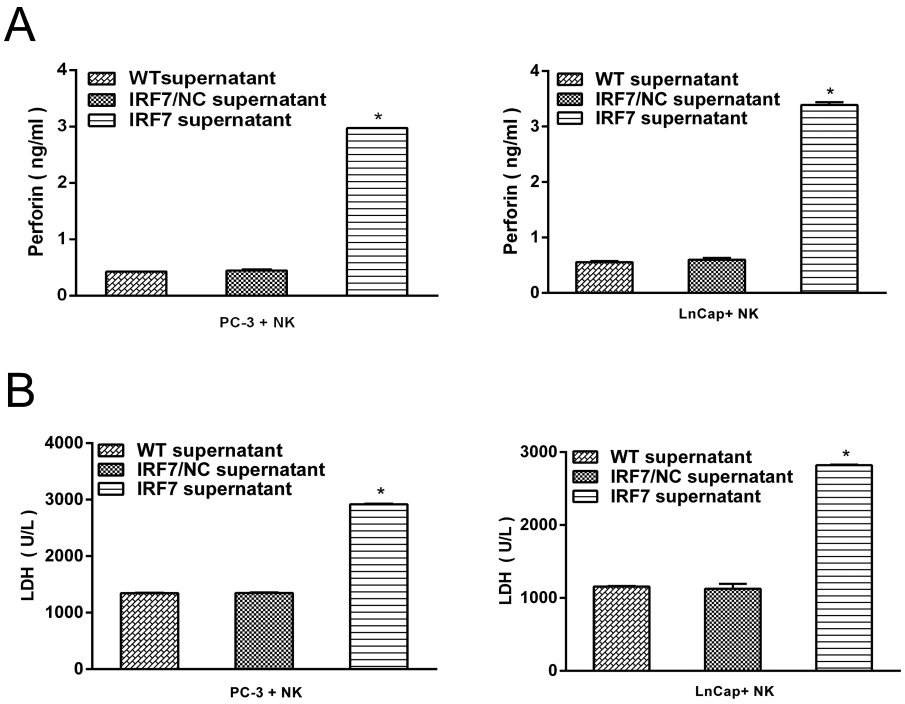

Figure 4. IRF7 regulated the activation of NK cells. (A) The expression of perforin-1 in the coculture system (prostate cancer cells and NK cells) was detected by ELISA. $*p<0.05$, respectively. (B) The expression of LDH in the coculture system (prostate cancer cells and NK cells) was detected by ELISA. $*p<0.05$.

and Transwell invasion assays were also conducted to assess the mobility and invasion ability of prostate cancer cells. Similarly, these data revealed that IRF7 overexpression could not change the mobility and invasion ability ($p>0.05$) (Fig. 3C and D). Taken together, these findings revealed that IRF7 had no effect on the malignant phenotype of prostate cancer cells, which might be consistent with previous results that showed IRF7 expression in prostate cancer tissues was not associated with the Gleason score.

IRF7-Activated NK cells

It is well documented that NK cells in nude mice played a role in inhibiting systemic metastasis of cancer cells, which provided putative evidence that NK cells might be involved in the inhibition of bone metastasis after excluding the direct effect of IRF7 on growth inhibition in prostate cancer. To identify the capacity of IRF7 to activate NK cells, a coculture system was developed, which contained 1×10^6 NK cells from healthy donors and 1×10^5 prostate cancer cells. Then the culture supernatant of prostate cancer cells overexpressing IRF7 was added into the coculture system. Twenty-four hours later, increased perforin-1 and LDH expression in the coculture supernatant were detected compared with the control group ($p<0.05$) (Fig. 4A and B). The data demonstrated that the culture supernatant of prostate cancer cells overexpressing IRF7 rapidly activated NK cells.

IFN-β Induced by IRF7 Involved in the Regulation of NK Activity

The expression of classic and putative prostate cancer-related cytokines including matrix metalloproteinases-9 (MMP-9), vascular endothelial growth factor A (VEGF-A), IL-6, type I IFN (IFN-α and IFN-β), and p53 in prostate cancer cells overexpressing IRF7 was evaluated. IFN-β

FACING PAGE

Figure 5. IFN-β involved in the regulation of NK activity. (A) qRT-PCR for the classic and putative prostate cancer-related cytokines (MMP-9, VEGF-A, IL-6, IFN-β, IFN-α, and p53) in prostate cancer cells overexpressing IRF7 was conducted. (B) ELISA for IFN-β in the culture supernatant of prostate cancer cells, and cells were transfected with si-RNA (si-147 and si-623) directed against control (si-NC). (C) The expression of perforin-1 in the coculture system (prostate cancer cells and NK cells) was detected by ELISA. (D) The expression of LDH in the coculture system was detected by ELISA. (E) The expression of IFN-β and perforin-1 in peripheral blood of nude mice was confirmed by ELISA. $*p < 0.05$

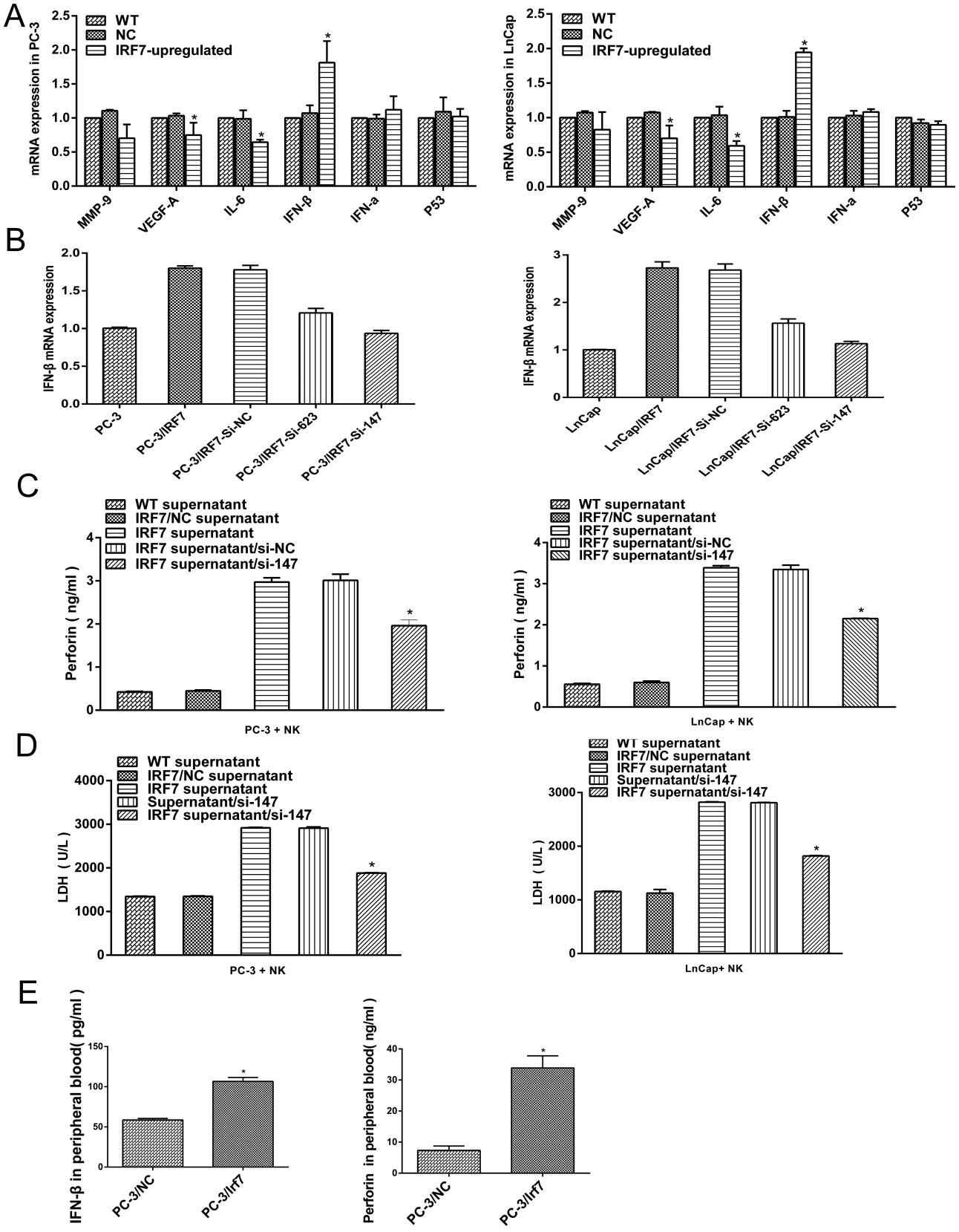
A
mRNA expression in PC-3
WT
NC
IRF7-upregulated
MMP-9
VEGF-A
IL-6
IFN-β
IFN-a
P53
mRNA expression in LnCap
B
IFN-β mRNA expression
PC-3
PC-3/IRF7
PC-3/IRF7-Si-NC
PC-3/IRF7-Si-623
PC-3/IRF7-Si-147
LnCap
LnCap/IRF7
LnCap/IRF7-Si-NC
LnCap/IRF7-Si-623
LnCap/IRF7-Si-147
C
WT supernatant
IRF7/NC supernatant
IRF7 supernatant
IRF7 supernatant/si-NC
IRF7 supernatant/si-147
Perforin (ng/ml)
PC-3 + NK
LnCap + NK
D
Supernatant/si-147
LDH (U/L)
PC-3 + NK
LnCap+ NK
E
IFN-β in peripheral blood(pg/ml)
PC-3/NC
PC-3/Irf7
Perforin in peripheral blood(ng/ml)

was the most obviously increased in prostate cancer cells (Fig. 5A). Hence, IFN-β signaling was chosen for further assays.

To investigate whether IRF7 regulates NK activity through IFN-β signaling, the expression of IFN-β in prostate cancer cells overexpressing IRF7 was downregulated by si-147, which exhibited the highest efficiency in knockdown of IFN-β (Fig. 5B), and the culture supernatant was added into the coculture system as mentioned above. The data showed that decreased perforin-1 and LDH in coculture supernatant were detected ($p<0.05$) (Fig. 5C and D), which provided a support that the activity of NK was suppressed due to the downregulation of IFN-β in the supernatant. Moreover, in further analysis on IFN-β and perforin-1 expression in the peripheral blood of nude mice with xenograft of the prostate cancer cells overexpressing IRF7, a high level of IFN-β and perforin-1 was confirmed by ELISA compared with the control ($p<0.05$) (Fig. 5E). Taken together, these results illustrated the role of IFN-β induced by IRF7 in the regulation of NK activity.

DISCUSSION

Prostate cancer bone metastasis is strongly associated with poor prognosis. Studies have identified certain biomarkers for predicting bone metastases of primary prostate cancer, such as TRACP, Id-4, BMP-6, CD44v6, collagen XXIII, etc.[13–17], but there has not been an efficient marker for predicting bone metastasis to date. Therefore, identifying an efficient marker in prostate cancer is necessary and helpful for high-risk patients who may benefit from appropriate therapeutic approaches to decrease the risk of bone metastasis.

The IRF7 gene was originally cloned in 1997, in the context of latent Epstein–Barr virus (EBV) infection where the encoded protein binds to and regulates the EBNA1 Q promoter[18]. In human angiomyolipoma (AML) cells 621.102 and 621.103, knockdown of IRF7 in the Rheb/mTOR pathway by si-RNA inhibited the proliferation of AML cells[19]. In addition, it has been reported that ectopic expression of IRF7 in human glioma cells U87MG and LN229 directly induced the production of IL-6, which maintained glioma stem cell properties via the Janus kinase/signal transducer and activator of transcription-mediated activation of Jagged-Notch signaling[9]. However, mounting evidence has shed light on the importance of IRF7 in antitumor properties. Besides, the direct effect of IRF7 on inhibition of growth and induction of senescence in immortal Li–Fraumeni fibroblasts[5] studies tended to support the role of IRF7-mediated immune response in cancer therapy. Adenovirus-mediated transduction of the active form of IRF7 into primary macrophages resulted in the production of type I IFN, upregulation of target genes including TRAIL, and increased tumoricidal activity of macrophages[20]. In breast cancer, IRF7-induced IFN-α production prevented the accumulation of myeloid-derived suppressor cells (MDSCs) and induced the activation of $CD4^+$, $CD8^+$, and NK cells, which was strongly involved in the inhibition of bone metastasis[8]. However, none of these studies has reported the function of IRF7 in prostate cancer bone metastasis. In our research, IRF7 protein was partially suppressed in bone metastases of prostate cancer by IHC, and Kaplan–Meier analysis showed that IRF7 alone or in combination with IFN-β has the predictive value for bone metastasis ($p=0.030$ and $p=0.001$, respectively). In addition, a series of in vitro and in vivo assays were employed to investigate the function of IRF7 in prostate cancer. The results showed that IRF7 substantially inhibited bone metastasis of prostate cancer cells in vivo but had no significant effect on the malignant phenotype of prostate cancer cells in vitro.

The mechanism involved in IRF7's regulation of prostate cancer bone metastasis is still unknown. IRF7 protein is a multifunctional transcription factor, underscored by the fact that it is the master regulator of type I IFN-dependent immune responses, which has proven that type I IFN (IFN-α and IFN-β) was a direct target of IRF7[4]. IFN-β belongs to the type I IFN group and functions as a tumor inhibitor in prostate cancer[21]. It has been further revealed that low-level expression of IFN-β is strongly related to biochemical recurrence of prostate cancer[22]. In our study, upregulation of IRF7 significantly increased the expression of IFN-β both in vitro and in vivo. This result is different from Bidwell's findings that IFN-α, but not IFN-β, was induced by IRF7 in breast cancer cells[8]. The mechanism of IRF7's regulation of prostate cancer bone metastasis required a specific activator for immune response, which can effectively activate immune cells.

NK cells are recognized as the key antimetastatic immune cells[23,24], which had strong cytotoxic activity against malignant tumor cells lacking MHC class I molecules and played an important role in the initiation of subsequent adaptive immunity. Previous studies demonstrated that NK cells were the essential mediators of the antimetastatic effects of a number of recombinant cytokines such as IL-2, IL-12, IL-18, and IL-21[25–27]. Remarkably, according to nude mice models, NK cells had a therapeutic effect against glioblastomas in the brain and inhibited the systemic metastasis of glioblastoma cells[23]. Moreover, the long-term survival of NK cells in the livers of nude mice also inhibited lung metastasis of hepatocellular carcinoma[24]. These results indicate the key role of NK cells in antimetastasis. On the other hand, studies have confirmed that type I IFNs are an early and critical regulator of NK-cell numbers and activation. Using both IFNAR1- and IFNAR2-deficient mice, endogenous

type I IFN exhibited a critical role in controlling NK cell-mediated antitumor responses in many experimental tumor models[28]. Our study thus demonstrated that IFN-β gene knockdown was involved in the suppression of NK-cell activity.

In conclusion, we identified the role of IRF7 in inhibiting bone metastasis of prostate cancer and revealed the novel signature that IRF7 alone or in combination with IFN-β might be a useful biomarker for bone metastasis of primary prostate cancer and the underlying mechanism may be associated with the increasing expression of IFN-β and the activation of NK cells. Further studies targeting the novel molecule IRF7 for the treatment of prostate cancer are recommended.

ACKNOWLEDGMENT: The authors declare no conflicts of interest.

REFERENCES

1. Beltran H, Beer TM, Carducci MA, de Bono J, Gleave M, Hussain M, Kelly WK, Saad F, Sternberg C, Tagawa ST, Tannock IF. New therapies for castration-resistant prostate cancer: Efficacy and safety. Eur Urol. 2011;60:279–90.
2. Eaton CL, Colombel M, van der Pluijm G, Cecchini M, Wetterwald A, Lippitt J, Rehman I, Hamdy F, Thalman G. Evaluation of the frequency of putative prostate cancer stem cells in primary and metastatic prostate cancer. Prostate 2010;70:875–82.
3. Sturge J, Caley MP, Waxman J. Bone metastasis in prostate cancer: Emerging therapeutic strategies. Nat Rev Clin Oncol. 2011;8:357–68.
4. Honda K, Yanai H, Negishi H, Asagiri M, Sato M, Mizutani T, Shimada N, Ohba Y, Takaoka A, Yoshida N, Taniguchi T. IRF-7 is the master regulator of type-I interferon-dependent immune responses. Nature 2005;434:772–7.
5. Li Q, Tang L, Roberts PC, Kraniak JM, Fridman AL, Kulaeva OI, Tehrani OS, Tainsky MA. Interferon regulatory factors IRF5 and IRF7 inhibit growth and induce senescence in immortal Li-Fraumeni fibroblasts. Mol Cancer Res. 2008;6:770–84.
6. Yang Y, Shaffer AL 3rd, Emre NC, Ceribelli M, Zhang M, Wright G, Xiao W, Powell J, Platig J, Kohlhammer H, Young RM, Zhao H, Yang Y, Xu W, Buggy JJ, Balasubramanian S, Mathews LA, Shinn P, Guha R, Ferrer M, Thomas C, Waldmann TA, Staudt LM. Exploiting synthetic lethality for the therapy of ABC diffuse large B cell lymphoma. Cancer Cell 2012;21:723–37.
7. Buckley NE, Hosey AM, Gorski JJ, Purcell JW, Mulligan JM, Harkin DP, Mullan PB. BRCA1 regulates IFN-gamma signaling through a mechanism involving the type I IFNs. Mol Cancer Res. 2007;5:261–70.
8. Bidwell BN, Slaney CY, Withana NP, Forster S, Cao Y, Loi S, Andrews D, Mikeska T, Mangan NE, Samarajiwa SA, de Weerd NA, Gould J, Argani P, Möller A, Smyth MJ, Anderson RL, Hertzog PJ, Parker BS. Silencing of Irf7 pathways in breast cancer cells promotes bone metastasis through immune escape. Nat Med. 2012;18:1224–31.
9. Jin X, Kim SH, Jeon HM, Beck S, Sohn YW, Yin J, Kim JK, Lim YC, Lee JH, Kim SH, Kang SH, Pian X, Song MS, Park JB, Chae YS, Chung YG, Lee SH, Choi YJ, Nam DH, Choi YK, Kim H. Interferon regulatory factor 7 regulates glioma stem cells via interleukin-6 and Notch signalling. Brain 2012;135:1055–69.
10. Kim JK, Jin X, Ham SW, Lee SY, Seo S, Kim SC, Kim SH, Kim H. IRF7 promotes glioma cell invasion by inhibiting AGO2 expression. Tumour Biol. 2015;36:5561–9.
11. Wei T, Liu Q, He F, Zhu W, Hu L, Guo L, Zhang J. The role of N-acetylglucosaminyltransferases V in the malignancy of human hepatocellular carcinoma. Exp Mol Pathol. 2012;93:8–17.
12. Wei T, Li Y, Zhuo E, Zhu W, Meng H, Zhang J. Down-regulation of GnT-V inhibits nasopharyngeal carcinoma cell CNE-2 malignancy in vitro and in vivo. Cancer Lett. 2011;309:151–61.
13. Ni J, Cozzi PJ, Hao JL, Beretov J, Chang L, Duan W, Shigdar S, Delprado WJ, Graham PH, Bucci J, Kearsley JH, Li Y. CD44 variant 6 is associated with prostate cancer metastasis and chemo-/radioresistance. Prostate 2014;74:602–17.
14. Banyard J, Bao L, Hofer MD, Zurakowski D, Spivey KA, Feldman AS, Hutchinson LM, Kuefer R, Rubin MA, Zetter BR. Collagen XXIII expression is associated with prostate cancer recurrence and distant metastases. Clin Cancer Res. 2007;13:2634–42.
15. Yuen HF, Chua CW, Chan YP, Wong YC, Wang X, Chan KW. Id proteins expression in prostate cancer: High-level expression of Id-4 in primary prostate cancer is associated with development of metastases. Mod Pathol. 2006;19:931–41.
16. Ozu C, Nakashima J, Horiguchi Y, Oya M, Ohigashi T, Murai M. Prediction of bone metastases by combination of tartrate-resistant acid phosphatase, alkaline phosphatase and prostate specific antigen in patients with prostate cancer. Int J Urol. 2008;15:419–22.
17. Yuen HF, Chan YP, Cheung WL, Wong YC, Wang X, Chan KW. The prognostic significance of BMP-6 signaling in prostate cancer. Mod Pathol. 2008;21:1436–43.
18. Zhang L, Pagano JS. IRF-7, a new interferon regulatory factor associated with Epstein-Barr virus latency. Mol Cell Biol. 1997;17:5748–57.
19. Makovski V, Jacob-Hirsch J, Gefen-Dor C, Shai B, Ehrlich M, Rechavi G, Kloog Y. Analysis of gene expression array in TSC2-deficient AML cells reveals IRF7 as a pivotal factor in the Rheb/mTOR pathway. Cell Death Dis. 2014;5:e1557.
20. Solis M, Goubau D, Romieu-Mourez R, Genin P, Civas A, Hiscott J. Distinct functions of IRF-3 and IRF-7 in IFN-alpha gene regulation and control of anti-tumor activity in primary macrophages. Biochem Pharmacol. 2006;72:1469–76.
21. Lee J, Wang A, Hu Q, Lu S, Dong Z. Adenovirus-mediated interferon-beta gene transfer inhibits angiogenesis in and progression of orthotopic tumors of human prostate cancer cells in nude mice. Int J Oncol. 2006;29:1405–12.
22. Eiro N, Bermudez-Fernandez S, Fernandez-Garcia B, Atienza S, Beridze N, Escaf S, Vizoso FJ. Analysis of the expression of interleukins, interferon beta, and nuclear factor-kappa B in prostate cancer and their relationship with biochemical recurrence. J Immunother. 2014;37:366–73.
23. Lee SJ, Kang WY, Yoon Y, Jin JY, Song HJ, Her JH, Kang SM, Hwang YK, Kang KJ, Joo KM, Nam DH. Natural killer (NK) cells inhibit systemic metastasis of glioblastoma cells and have therapeutic effects against glioblastomas in the brain. BMC Cancer 2015;15:1011.
24. Hong ZF, Zhao WX, Yin ZY, Xie CR, Xu YP, Chi XQ, Zhang S, Wang XM. Natural killer cells inhibit pulmonary

metastasis of hepatocellular carcinoma in nude mice. Oncol Lett. 2016;11:2019–26.
25. Brady J, Hayakawa Y, Smyth MJ, Nutt SL. IL-21 induces the functional maturation of murine NK cells. J Immunol. 2004;172:2048–58.
26. Smyth MJ, Swann J, Kelly JM, Cretney E, Yokoyama WM, Diefenbach A, Sayers TJ, Hayakawa Y. NKG2D recognition and perforin effector function mediate effective cytokine immunotherapy of cancer. J Exp Med. 2004;200: 1325–35.
27. Smyth MJ, Taniguchi M, Street SE. The anti-tumor activity of IL-12: Mechanisms of innate immunity that are model and dose dependent. J Immunol. 2000;165:2665–70.
28. Swann JB, Hayakawa Y, Zerafa N, Sheehan KC, Scott B, Schreiber RD, Hertzog P, Smyth MJ. Type I IFN contributes to NK cell homeostasis, activation, and antitumor function. J Immunol. 2007;178:7540–9.